
Article:
Becque, J. (2016) The application of plastic flow theory to inelastic column buckling. International Journal of Mechanical Sciences, 111. pp. 116-124. ISSN: 1879-2162

https://doi.org/10.1016/j.ijmecsci.2016.04.005

THE APPLICATION OF PLASTIC FLOW THEORY TO INELASTIC COLUMN BUCKLING

by Jurgen Becque[1]

ABSTRACT

The paper presents a theory of inelastic column buckling which is consistent with the principles of plastic flow theory. The theory accounts for flexural, torsional and flexural-torsional modes. While the use of the tangent modulus to describe inelastic flexural buckling has been common place for a long time, efforts to comprehensively unite the torsional and flexural-torsional modes with the principles of plastic flow theory have so far been hampered by the 'plastic buckling paradox'. New theoretical developments presented in this paper provide a way to achieve this goal. The solution hinges on the derivation of the inelastic shear stiffness while considering an infinitesimal solid element embedded within the column at a stage immediately past the point of buckling.

The proposed inelastic column theory is verified against selected experimental data pertaining to aluminium and stainless steel columns of various cross-sections. Particular attention is paid to the torsional buckling problem of the inelastic cruciform section column.

[1]Lecturer, Department of Civil and Structural Engineering, University of Sheffield, Sir Frederick Mappin Building, Mappin Street, S1 3JD Sheffield, UK. Tel: +44 (0)114 2220252, J.Becque@Sheffield.ac.uk

1. BACKGROUND

With respect to inelastic flexural buckling of columns, Engesser (1889) was the first to propose the use of the tangent modulus E_t to predict the buckling load of an initially perfectly straight, inelastic column by modifying Euler's differential equation as follows:

$$E_t I \frac{d^2 u}{dx^2} + Pu = 0 \tag{1}$$

where u is the lateral column deflection, P is the axial compressive load and I is the second moment of area of the cross-section about the principal axis about which bending takes place. Eq. (1) results in an expression for the column buckling load:

$$P_{cr} = \pi^2 \frac{E_t I}{L_e^2} \tag{2}$$

where L_e is the effective length, dependent on the boundary conditions.

While straightforward, Engesser's approach received criticism from Considère (1891) who argued that, as the column starts to bend out laterally, elastic unloading takes place on the convex side of bending and that consequently, the bending stiffness is not simply determined by $E_t I$. Engesser (1895) replied by proposing his "double-modulus" or "reduced modulus" theory, where:

$$P_{cr} = \pi^2 \frac{E_r I}{L_e^2} \tag{3}$$

with:

$$E_r = E_t \frac{I_c}{I} + E_0 \frac{I_t}{I} \tag{4}$$

I_c and I_t are the second moments of area of the parts of the cross-section subjected to compression and tension with respect to the neutral axis, respectively, and E_0 is the initial elastic modulus.

It soon became apparent that Eq. (2) showed much better agreement with the experiment than Eq. (3), which consistently led to overestimates. Shanley (1947) shed light on this seeming paradox by pointing out that Eq. (2) does indeed constitute the buckling load of the column since it indicates the point of bifurcation above which the column cannot be in a state of stable equilibrium while remaining straight. Moreover, lateral buckling does not take place under a constant load, but elastic unloading on the convex side instead results in postbuckling capacity.

A realistic theory describing buckling of inelastic columns involving torsion, which may either occur as pure torsional buckling or combined flexural and torsional buckling, based on the principles of plastic flow theory has not yet been presented. The challenge thereby lies in modelling the relationship between increments of shear stress and shear strain at the onset of buckling. A previous interpretation of plastic flow theory (Hutchinson 1974, Lubliner 1990, Bazant and Cedolin 1991) has suggested that the increments of shear stress

and shear strain remain linked through the elastic modulus E_0 at the onset of buckling and that, therefore, the torsional resistance remains unaffected by the axially induced plasticity. This conclusion, however, stands in clear contradiction with experimental observations, as demonstrated by, among others, Batdorf (1949), Onat and Drucker (1952), Hutchinson (1974), Lubliner (1990) and Bazant and Cedolin (1991). This "plastic buckling paradox", as it is often named in literature, is particularly exemplified by the torsional buckling problem of the inelastic cruciform column, since this particular cross-section relies on the shear stresses resulting from pure torsion to a much larger extent than on the (negligible) longitudinal warping stresses in its buckling resistance. Experiments on cruciform sections have indicated that plastic flow theory substantially overestimates the buckling load. On the other hand, buckling theories based on plastic deformation theory, which is generally considered flawed and inferior in its concept to plastic flow theory, have so far yielded the better predictions in relation to column buckling problems involving torsion. This is more generally true for inelastic bifurcation problems and this paradoxical issue continues to hamper theoretical stability research, as demonstrated recently by, for instance, Rønning et al. (2010) for plates, Shamass et al. (2015) for cylindrical shells and Ruocco (2015) for instabilities in thin-walled elements in general. The plastic buckling paradox has also been excellently illustrated for thick and thin plates under uniaxial, biaxial and shear loading by Wang et al. (2001), Wang and Tun Myint Aung (2007) and Wang and Huang (2009). The problem also arises within the context of Generalized Beam Theory (GBT), as demonstrated by Gonçalves and Camotim (2007). The authors developed two GBT formulations, incorporating either deformation theory or flow theory. These new

formulations were then applied to the cases of simple plates under uniform compression and hat section beams in uniform bending. It was concluded that the flow-based GBT resulted in much higher predictions of the buckling stresses than the deformation-based theory.

Interestingly, it has been observed (Shamass 2015) that the results of geometrically non-linear finite element analyses using flow theory with an associated flow rule are unaffected by the plastic buckling paradox. While no explanation has yet been provided as to why an incremental numerical approach remedies the problem, a firm conclusion can be drawn from this observation, namely that the plastic buckling paradox is not due to any inherent shortcomings or limitations of flow theory itself, but rather a result of an incorrect application of its principles. This idea is central to the theory proposed in this paper.

Onat and Drucker (1953) demonstrated that the plastic buckling paradox can be circumvented by incorporating imperfections into the model and that even very small, inevitable imperfections have a severe impact on the buckling load, reducing it to levels close to those predicted by deformation theory. Hutchinson and Budiansky (1976) confirmed this finding for low strain-hardening metals. However, they also demonstrated that for metals with significant strain-hardening the imperfections have to be of such magnitude that they can no longer be considered ‘small and inevitable’, thus suggesting that Onat and Drucker’s explanation is not entirely satisfying.

The approach presented in this paper differs from the aforementioned rationale in that a perfectly straight column is considered, without initial imperfections. Instead, the plastic buckling paradox is resolved by deriving a relationship between shear stress and shear

strain increments at the onset of buckling, while applying the plastic flow rule to a solid element in its shear deformed shape. The basic principles of plastic flow theory, however, are retained.

2. INELASTIC SHEAR STIFFNESS

An expression for the inelastic shear stiffness G_1 of a non-linear metal is first derived, accounting for the presence of a uniaxial compressive stress. G_1 will be used in the following paragraphs to relate increments of shear stress and shear strain at the point of column buckling. The derivation here presented is a generalized and amended version of the one contained in Becque (2010).

We consider the material stress-strain curve of a non-linear metal, as determined from a uniaxial compression test (Fig. 1). It is a generally accepted postulate of plasticity that an increment in axial strain $\dot{\varepsilon}_1$ is composed of an reversible elastic component $\dot{\varepsilon}_{1,el}$ and an irreversible plastic component $\dot{\varepsilon}_{1,p}$:

$$\dot{\varepsilon}_1 = \dot{\varepsilon}_{1,el} + \dot{\varepsilon}_{1,p} \tag{5}$$

Eq. (5) can be written in terms of the increment in axial stress $\dot{\sigma}_1$ associated with $\dot{\varepsilon}_1$:

$$\frac{\dot{\sigma}_1}{E_t} = \frac{\dot{\sigma}_1}{E_0} + \frac{\dot{\sigma}_1}{E_p} \tag{6}$$

where E_0 is the elastic modulus, E_t is the tangent modulus at the relevant stress level and E_p relates the plastic stress and strain increments. Thus:

$$\frac{1}{E_p} = \frac{1}{E_t} - \frac{1}{E_0} \tag{7}$$

Plastic flow theory also dictates that the incremental plastic strain in the perpendicular principal 2-direction is given by:

$$\dot{\varepsilon}_{2,P} = \kappa \dot{\varepsilon}_{1,P} \tag{8}$$

An associated flow rule is adopted, so that κ in Eq. (8) is determined by the slope of the normal to the flow surface (Drucker 1950). When the von Mises surface is used (Fig. 2), κ amounts to -1/2 under uniaxial compression. However, the calculations will carry a general κ value to allow for possible plastic anisotropy in the material.

Figure 3a depicts an infinitesimal element of material embedded within the column wall at a certain depth in the thickness direction. Up to the point of buckling, the principal 1-direction of stress coincides with the longitudinal axis of the column, while we orient the 2-direction in the tangential direction along the heart line of the cross-section. When the axially applied stress reaches a critical stress σ_{cr} with respect to the torsional or flexural-torsional buckling mode, a further stress increment $\dot{\sigma}_1$ will cause the infinitesimal element

to undergo incremental deformations in the 1- and 2-directions, as well as deformations in shear characterized by the angles $\dot{\theta}_1$ and $\dot{\theta}_2$ in Figure 3a. The angles $\dot{\theta}_1$ and $\dot{\theta}_2$ are, in general, different as the infinitesimal element may also undergo a rigid body rotation relative to the direction of the axial stress in addition to its shear deformations. The load on the column is thereby assumed to be a gravity load or similar to a gravity load in a sense that it maintains its vertical direction in space as the column buckles.

It is noted that the classical formulation of flow theory does not predict any plastic shear deformations to take place in this process (Hutchinson 1974, Lubliner 1990, Bazant and Cedolin 1991). In other words, the incremental shear deformations are purely elastic. However, this point of view can be dislodged by considering the infinitesimal plate element in its deformed shape (Figure 3a) in combination with Mohr's circle of the *incremental plastic* strains (Figure 3b). For completeness, a few notes should be added. First, the incremental plastic deformation in the thickness direction, $\dot{\varepsilon}_{3,p}$, is non-zero. However, since the 3-direction constitutes a principal direction and is also the axis of rotation of our reference system, the use of Mohr's circle is indeed justified. Second, plastic flow theory dictates that the principal directions of the incremental plastic strains coincide with the principal directions of the (total) stresses. At the point of buckling, infinitesimal plate bending stresses and shear stresses develop. However, since these additional stresses are initially infinitesimal, they do not affect the principal directions of stress. For the purpose of considering the incremental step in Figure 3 immediately past the point of buckling, the principal directions of stress (and thus of incremental plastic strain) remain firmly pointed along the column axis and in the perpendicular direction within the column wall.

While the infinitesimal plate element in Figure 3a deforms, the sides a-a and b-b rotate from their initial vertical and horizontal positions to final inclined positions at the end of the load increment. At any stage during this transition, Mohr's circle indicates the magnitude of plastic shearing which occurs along a-a and b-b. It is clear that, while planes a-a and b-b rotate, the instantaneous magnitudes of the shear strains along a-a and b-b (which are initially zero) gradually increase. The total plastic strain increments need therefore be found by incremental integration, where the total increment in principal plastic strain $\dot{\varepsilon}_{1,p}$ is subdivided into a number of intervals $\left(\dot{\varepsilon}_{1,p}/\dot{\theta}_1\right)d\alpha$. The sum of the $d\alpha$'s thereby adds up to $\dot{\theta}_1$. In each interval the radius of Mohr's circle is given by:

$$R = \frac{(1-\kappa)}{2}\frac{\dot{\varepsilon}_{1,p}}{\dot{\theta}_1}d\alpha \qquad (9)$$

Therefore, the total plastic shear strains along a-a and b-b at the end of the increment are found as follows:

$$\dot{\varepsilon}_{a,p} = \int_{\alpha=0}^{\alpha=\dot{\theta}_1}\frac{(1-\kappa)}{2}\frac{\dot{\varepsilon}_{1,p}}{\dot{\theta}_1}\sin 2\alpha\, d\alpha = -\frac{1}{2}\frac{(1-\kappa)}{2}\frac{\dot{\varepsilon}_{1,p}}{\dot{\theta}_1}\left(\cos 2\dot{\theta}_1 - 1\right) \approx \frac{(1-\kappa)}{2}\dot{\theta}_1\dot{\varepsilon}_{1,p} \qquad (10)$$

$$\dot{\varepsilon}_{b,p} = -\int_{\alpha=0}^{\alpha=\dot{\theta}_2}\frac{(1-\kappa)}{2}\frac{\dot{\varepsilon}_{1,p}}{\dot{\theta}_2}\sin 2\alpha\, d\alpha = \frac{1}{2}\frac{(1-\kappa)}{2}\frac{\dot{\varepsilon}_{1,p}}{\dot{\theta}_2}\left(\cos 2\dot{\theta}_2 - 1\right) \approx -\frac{(1-\kappa)}{2}\dot{\theta}_2\dot{\varepsilon}_{1,p} \qquad (11)$$

Eqs. (10-11) use the fact that, since Fig. 3a represents a state immediately past the point of buckling, the angles $\dot{\theta}_1$ and $\dot{\theta}_2$ are necessarily small.

The increment in axial stress $\dot{\sigma}_1$ causes incremental shear stresses along the sides a-a and b-b which, given the state of plane stress, can be determined using Mohr's circle for the incremental stresses (Fig. 3c):

$$\dot{\tau}_a = \frac{\dot{\sigma}_1}{2}\sin 2\dot{\theta}_1 \approx \dot{\sigma}_1\dot{\theta}_1 \tag{12}$$

$$\dot{\tau}_b = -\frac{\dot{\sigma}_1}{2}\sin 2\dot{\theta}_2 \approx -\dot{\sigma}_1\dot{\theta}_2 \tag{13}$$

When a stress increment $\dot{\sigma}_1$ is applied in the axial direction of the column, the material responds with a tangent stiffness E_t which is dependent on the stress level σ_1 and which can be determined from the uniaxial stress-strain curve. At the point of buckling the strain hardening rule can therefore be written (with the help of Eq. 7) as:

$$\dot{\varepsilon}_{1,p} = \frac{\dot{\sigma}_1}{E_p} = \dot{\sigma}_1\left[\frac{1}{E_t} - \frac{1}{E_0}\right] \tag{14}$$

Using Eq. (14) the angles $\dot{\theta}_1$ and $\dot{\theta}_2$ can be eliminated from Eqs. (9-10) and Eqs. (12-13):

$$\dot{\varepsilon}_{a,p} = \frac{(1-\kappa)}{2E_p}\dot{\tau}_a \tag{15}$$

$$\dot{\varepsilon}_{b,p} = \frac{(1-\kappa)}{2E_p}\dot{\tau}_b \qquad (16)$$

The constitutive equations (15-16) are independent of the angles $\dot{\theta}_1$ and $\dot{\theta}_2$ (within small perturbations of the unbuckled state) and, by consequence, have to hold true at the point of buckling itself. At this limit point, when the column is in an undeformed state (apart from an axial shortening), the angles $\dot{\theta}_1$ and $\dot{\theta}_2$ are zero and the planes a-a and b-b in Fig. 3 are perpendicular to each other. However, Eqs. (15-16) are still valid. In this undeformed state, reciprocity of the shear stresses holds, and thus: $\dot{\tau}_a = \dot{\tau}_b = \dot{\tau}$, while the total plastic shear straining can determined by adding Eqs. (15-16) (something which is, of course, not possible in the deformed state):

$$\dot{\gamma}_p = \dot{\varepsilon}_{a.p} + \dot{\varepsilon}_{b.p} = \frac{(1-\kappa)}{E_p}\dot{\tau} \qquad (17)$$

The elastic shear strain is governed by the well-known equation:

$$\dot{\gamma}_{el} = \frac{\dot{\tau}}{G_0} \qquad (18)$$

where G_0 is the elastic shear modulus: $G_0 = E_0/[2(1+\nu)]$.

The total shear strain increment is then given by:

$$\dot{\gamma} = \dot{\gamma}_{el} + \dot{\gamma}_{p} = \left(\frac{1}{G_0} + \frac{1-\kappa}{E_p} \right) \dot{\tau} \tag{19}$$

Using Eq. (7) to eliminate E_p yields the equation:

$$\dot{\tau} = \frac{E_t E_0}{(1+\kappa+2\nu)E_t + (1-\kappa)E_0} \dot{\gamma} \tag{20}$$

The inelastic shear modulus G_1, valid at the point of buckling, is thus given by:

$$G_1 = \frac{E_t E_0}{(1+\kappa+2\nu)E_t + (1-\kappa)E_0} \tag{21}$$

3. DIFFERENTIAL EQUATIONS

The differential equations describing the stability of an *elastic* thin-walled column without imperfections have been presented by Timoshenko (1945) (*see also* Timoshenko and Gere 1961), based on earlier work by Kappus (1937), Wagner and Pretschner (1936), Bleich and Bleich (1936), and Goodier (1942):

$$M_x = E_0 I_x \frac{d^2 v}{dz^2} = -P(v - x_0 \phi) \tag{22}$$

$$M_y = E_0 I_y \frac{d^2 u}{dz^2} = -P(u + y_0 \phi) \tag{23}$$

$$E_0 C_\omega \frac{d^4 \phi}{dz^4} - \left(G_0 J - \frac{I_p}{A} P \right) \frac{d^2 \phi}{dz^2} - P x_0 \frac{d^2 v}{dz^2} + P y_0 \frac{d^2 u}{dz^2} = 0 \tag{24}$$

In the above equations, the z-axis has been chosen to coincide with the longitudinal axis of the column, while the x- and y-axes are the principal axes within the cross-section (Fig. 4). The displacements u and v are those of the shear centre in the x- and y-directions, respectively, while the angle ϕ measures the rotation of the cross-section about the longitudinal axis through the shear centre. Furthermore, x_0 and y_0 are the coordinates of the shear centre relative to the centroid C, P is the axial load, I_x and I_y are the second moments of area about the x- and y-axes, respectively, C_ω is the warping constant, J is the torsional constant, A is the cross-sectional area, and I_p is the polar moment of area:

$$I_P = I_x + I_y + A(x_0^2 + y_0^2) \tag{25}$$

When considering bifurcation of an *inelastic* column, the torsional resistance associated with pure St. Venant torsion is governed by shear stresses which are linked to the shear strains by the inelastic modulus G_1, as determined by Eq. (21). Therefore, the torsional rigidity G_0J in Eq. (24) needs to be replaced by G_1J for an inelastic column. A second contribution to the torsional resistance results from the development of longitudinal warping stresses in non-uniform torsion. In an inelastic material, the longitudinal stress and

strain increments at the onset of buckling are related through the tangent modulus E_t. Therefore, the warping resistance of an inelastic column at the onset of buckling is governed by $E_t C_\omega$.

Furthermore, at the buckling load the longitudinal stress and strain increments due to bending are also linked by the tangent modulus E_t. Shanley's insights (1947) thereby indicate that no elastic unloading on the convex side of bending must be considered.

Based on these considerations, the differential equations describing stability of an inelastic column can now be written as:

$$E_t I_x \frac{d^2 v}{dz^2} + P\left(v - x_0 \phi\right) = 0 \tag{26}$$

$$E_t I_y \frac{d^2 u}{dz^2} + P\left(u + y_0 \phi\right) = 0 \tag{27}$$

$$E_t C_\omega \frac{d^4 \phi}{dz^4} - \left(G_t J - \frac{I_p}{A} P \right) \frac{d^2 \phi}{dz^2} - P x_0 \frac{d^2 v}{dz^2} + P y_0 \frac{d^2 u}{dz^2} = 0 \tag{28}$$

3. COLUMNS WITH A DOUBLY SYMMETRIC CROSS-SECTION

For columns with a doubly symmetric cross-section, the centroid and the shear centre coincide, so that: $x_0 = y_0 = 0$, and: $I_p = I_x + I_y$. Eqs. (26-28) now become a set of uncoupled differential equations:

$$E_t I_x \frac{d^2 v}{dz^2} + P v = 0 \tag{29}$$

$$E_t I_y \frac{d^2 u}{dz^2} + Pu = 0 \tag{30}$$

$$E_t C_\omega \frac{d^4 \phi}{dz^4} - \left(G_1 J - \frac{I_p}{A} P \right) \frac{d^2 \phi}{dz^2} = 0 \tag{31}$$

For a pin-ended column where the end sections are free to warp, but prevented from rotating about the longitudinal column axis, the boundary conditions are:

$$u = v = \phi = 0 \qquad \text{for} \qquad z = 0,\ z = L$$

$$\frac{d^2 u}{dz^2} = \frac{d^2 v}{dz^2} = \frac{d^2 \phi}{dz^2} = 0 \qquad \text{for} \qquad z = 0,\ z = L \tag{32}$$

Adopting the boundary conditions (32), the solution of Eqs. (26-28) is (*see* Timoshenko and Gere 1961):

$$P_x = \pi^2 \frac{E_t I_x}{L^2} \tag{33}$$

$$P_y = \pi^2 \frac{E_t I_y}{L^2} \tag{34}$$

$$P_\phi = \frac{A}{I_p}\left(G_1 J + E_t C_\omega \frac{\pi^2}{L^2}\right) \tag{35}$$

3.1 Flexural Buckling

Eqs. (33) and (34), of course, do not represent new findings. Originally proposed by Engesser (1889), the use of the tangent modulus to determine the pure flexural buckling load of columns is widely used and accepted. Although elastic unloading at the convex side of bending results in post-buckling capacity (Shanley 1947), this post-buckling capacity is usually marginal for non-linear metals as a result of the rapid loss of stiffness at higher strain levels. Consequently, the tangent modulus approach has been demonstrated to yield good predictions of the ultimate capacity of columns failing in flexural buckling. Research confirming this finding has been carried out by, among others, Osgood and Holt (1938), Leary and Holt (1946), Holt and Leary (1946), Johnson and Winter (1966), Rasmussen and Hancock (1993) and van den Berg (2000). The aforementioned research includes test on various aluminium and stainless steel alloys and encompasses columns of various cross-sections.

Heimerl and Roy (1945) conducted tests on extruded 75S-T aluminium "thin-strip" columns with rectangular cross-section. These particular tests are here used to illustrate Eq. (34). Figure 5 compares the reported data to Eq. (34), where a Ramberg-Osgood representation (Ramberg and Osgood 1943) of the stress-strain curve was used to calculate the tangent modulus:

$$E_t = \frac{\sigma_{0.2\%} E_0}{\sigma_{0.2\%} + 0.002 n E_0 \left(\frac{\sigma}{\sigma_{0.2\%}} \right)^{n-1}} \tag{36}$$

In Eq. (36), $\sigma_{0.2\%}$ is the 0.2% proof stress of the material and n is the strain-hardening parameter. For the material under consideration: E_0 = 72.5 GPa, $\sigma_{0.2\%}$ = 534 MPa and n = 22, as determined from the provided stress-strain curves in Heimerl and Roy (1945). Iterative calculations are necessary to solve Eq. (34). It is seen from Figure 5 that Eq. (34), representing the flexural buckling load of a perfectly straight column, constitutes an upper bound to the experimental data, which include the effects of initial imperfections.

3.2 Pure Torsional Buckling

Doubly symmetric sections with low torsional rigidity may be subject to a pure torsional buckling mode. The proposed theory is here verified against experimental data by Hopperstad et al. (1999), who conducted torsional buckling tests on extruded AA6082-T4 aluminium cruciform columns. Tests were conducted for five b/t ratios (see Figure 6 for a definition of b and t), while the L/b ratio (with L representing the column length) was kept constant at 6. The out-of-flatness of the flanges was reported to be less than 0.005b. All columns were tested between fixed end plates, so that warping of the end sections was prevented. The boundary conditions for torsion can thus be expressed as:

$$\phi = 0 \qquad \text{and} \qquad \frac{d\phi}{dz} = 0 \qquad \text{for} \qquad z = 0,\ z = L \tag{37}$$

which results in the replacement of Eq. (35) by (Timoshenko and Gere 1961):

$$P_\phi = \frac{A}{I_p}\left(G_1 J + E_t C_\omega \frac{4\pi^2}{L^2}\right) \tag{38}$$

The inelastic shear modulus G_1 was calculated using Eq. (21) with $\nu = 0.33$, $\kappa = -0.5$ and with the tangent modulus E_t determined by Eq. (36). The material parameters of the AA6082-T4 alloy, as reported by Hopperstad et al. (1999), are: $E_0 = 69.7$ GPa, $\sigma_{0.2\%} = 131$ MPa and $n = 23$. Since the heart lines of the constituent plate elements of the cross-section intersect at the shear centre, the classical theory of torsion (*see* Timoshenko and Gere 1961) dictates that $C_\omega = 0$, leaving only the contribution of pure torsion in Eq. (35):

$$\sigma_{cr} = \frac{P_\phi}{A} = \frac{G_1 J}{I_p} = G_1 \frac{4bt^3/3}{4b^3 t/3} = G_1\left(\frac{t}{b}\right)^2 \tag{39}$$

However, a more accurate approach originates from the realization that torsional buckling of the cruciform column is synonymous with local buckling of the four constituent flanges as plates simply supported along one longitudinal edge, with the other longitudinal edge

free (Figure 6), and that consequently longitudinal bending stresses develop in the flanges during torsional buckling. These bending stresses implied by plate theory are indeed equivalent to the warping stresses in the context of column theory. This allows for a more accurate determination of C_ω by noting that, if transverse plate bending is neglected (Figure 7):

$$v(x,z) = \phi(z).x \tag{40}$$

and that the moment per unit plate width M_x is given by:

$$M_x = E_t \frac{t^3}{12}\frac{d^2v}{dz^2} = E_t \frac{t^3}{12}\frac{d^2\phi}{dz^2}x \tag{41}$$

Consequently, the shear force per unit plate width V_x is given by:

$$V_x = \frac{dM_x}{dz} = E_t \frac{t^3}{12}\frac{d^3\phi}{dz^3}x \tag{42}$$

And the associated torsional moment is:

$$T_2 = -4\int_0^b V_x x\, dx = -E_t \frac{b^3t^3}{9}\frac{d^3\phi}{dz^3} \tag{43}$$

which yields:

$$C_{\omega} = \frac{b^3 t^3}{9} \tag{44}$$

A slightly more accurate equation can be obtained by replacing Eq. (41) by the expression for M_x obtained from inelastic plate theory (Becque 2010), while maintaining the displacement field proposed by Eq. (40):

$$M_x = \frac{t^3}{12}\frac{E_0 E_t}{(1+\nu\kappa)E_0 - \nu(\nu+\kappa)E_t}\left(\frac{\partial^2 v}{\partial z^2} + \nu\frac{\partial^2 v}{\partial x^2}\right) = \frac{t^3}{12}\frac{E_0 E_t}{(1+\nu\kappa)E_0 - \nu(\nu+\kappa)E_t}\frac{d^2\phi}{dz^2}x \tag{45}$$

The corresponding shear force is:

$$V_x = \frac{\partial M_x}{\partial z} + \frac{\partial M_{yx}}{\partial x}, \tag{46}$$

where $M_{yx} = 0$ as a result of Eq. (40).

Eq. (38) then becomes:

$$\sigma_{cr} = \frac{P_{\phi}}{A} = G_1\left(\frac{t}{b}\right)^2 + \frac{E_0 E_t}{(1+\nu\kappa)E_0 - \nu(\nu+\kappa)E_t}\frac{\pi^2}{3}\left(\frac{t}{L}\right)^2 \tag{47}$$

Since the warping resistance of the cruciform section is a priori small, Eq. (47) leads to predictions which differ by less than 0.5% from the results of Eq. (38), combined with Eq. (44), for the examples here considered.

Figure 8 plots the experimental results reported by Hopperstad et al. (1999) and compares them with the predictions of Eq. (38), using Eq. (44) to calculate C_ω. Iterative calculations are again necessary to solve Eq. (38). Good agreement between the predicted and the experimentally measured buckling stresses is obtained: the average ratio of the predicted to the measured buckling stress is 0.98. For comparison, Figure 8 also displays Ilyushin's (1947) solution for the buckling problem of a cruciform column, which is based on plastic deformation theory:

$$\sigma_{cr} = \frac{E_t}{3}\left[\frac{4\pi^2}{3}\left(\frac{b}{L}\right)^2 + \frac{E_s}{E_t}\right]\left(\frac{t}{b}\right)^2 \qquad (48)$$

where E_s is the secant modulus.

On a related note, it is seen from the experimental data that, since plates possess significant post-buckling capacity, the ultimate stress of the cruciform columns can considerably outreach the buckling stress. This is particularly true for the longer specimens, which buckle elastically.

Figure 9 compares the experimental data of Hopperstad et al. (1999) to two alternate solutions, the first of which was obtained from inelastic plate theory (Becque 2010), while the second one resulted from applying Eq. (39). With respect to Eq. (39), it is noted that the

omitted term in Eq. (38) becomes smaller for smaller values of E_t (meaning larger stresses and thus smaller b/t values), but on the other hand increases for larger C_ω/L^2 values (which also means smaller b/t values in Fig. 9, since the aspect ratio b/L is fixed). Which effect will dominate depends on the material stress-strain curve. With respect to the solution obtained from inelastic plate theory, each flange is regarded as a plate simply supported along three edges with one longitudinal edge free. Neither theory accounts for the slight rotational end restraint present in the experiments, which becomes relatively more important for longer specimens. On the other hand, for very short columns, plate theory yields better predictions over Eq. (38) because column theory fails to account for the transverse plate bending, which becomes important in shorter specimens.

4. COLUMNS WITH A SINGLY SYMMETRIC CROSS-SECTION

If the x-axis is an axis of symmetry, then: $y_0 = 0$, and Eqs. (26-28) become:

$$E_t I_y \frac{d^2u}{dz^2} + Pu = 0 \tag{49}$$

$$E_t I_x \frac{d^2v}{dz^2} + P(v - x_0\phi) = 0 \tag{50}$$

$$E_t C_\omega \frac{d^4\phi}{dz^4} - \left(G_t J - \frac{I_p}{A} P \right) \frac{d^2\phi}{dz^2} - P x_0 \frac{d^2v}{dz^2} = 0 \tag{51}$$

The flexural buckling mode about the y-axis, described by Eq. (49), which is dependent on u, is uncoupled from the flexural-torsional buckling mode in the y-direction, described by Eqs. (50-51), which contain v and ϕ. If the column ends are free to rotate about the x- and y-axes, but prevented from warping and rotating about the longitudinal axis, the flexural-torsional buckling load P is determined by the equation (*see* Timoshenko and Gere 1961):

$$\frac{I_x + I_y}{I_p} P^2 - \left(P_x + P_\phi\right)P + P_x P_\phi = 0 \tag{52}$$

where P_x and P_ϕ are given by Eqs. (33) and (38) respectively. Consequently:

$$P = \frac{I_p}{2\left(I_x + I_y\right)}\left[P_x + P_\phi - \sqrt{\left(P_x + P_\phi\right)^2 - 4P_x P_\phi \frac{I_x + I_y}{I_p}} \right] \tag{53}$$

Eq. (53) is first verified against experimental data provided by Leary and Holt (1946). The researchers tested equal-leg angles with dimensions 63.5mm x 63.5mm x 6.35mm, manufactured by extrusion of 14S-T aluminium. The reported material properties are: E_0 = 73.1 GPa, $\sigma_{0.2\%}$ = 394 MPa, n = 27 and ν = 0.33. The overall imperfections were reported to be less than L/1000. Using Eq. (44), the warping constant C_ω was calculated as:

$$C_\omega = \frac{b^3 t^3}{18} \tag{54}$$

Figure 10 compares the experimental data to the theoretical predictions. Iterative calculations are necessary to solve Eq. (53). The theory confirms the experimental observation that the longer columns fail by flexural buckling about the weak principal axis of the angle, while the shorter columns fail by flexural-torsional buckling. A close match between the theory and the experiment is obtained, with an average ratio of the predicted to the measured load of 1.00 for the specimens failing by flexural-torsional buckling. It should be noted that the test data represent ultimate (failure) stresses, while the theory predicts buckling stresses. The close match suggests that post-buckling capacity is limited for this type of inelastic buckling.

Secondly, Eq. (53) is verified against tests on 3Cr12 stainless steel hat section columns, failing by flexural-torsional buckling (van den Berg 1988). The material properties, as reported by van den Berg are: E_0 = 222 GPa, $\sigma_{0.2\%}$ = 319 MPa and n = 6.3. The cross-sectional dimensions are shown in Fig. 11. Figure 12 compares the results of Eq. (53) with the experimental data in dashed line. It is seen that the capacity of the shorter specimens significantly exceeds the predictions. The difference can be attributed to the fact that the sections were cold-formed, resulting in significantly increased corner properties (*see*, among others, Lecce 2006, Becque 2009). Due to the location of the corners with respect to the principal axes, the enhanced corner areas considerably increase the effective second moment of area I_y, while also improving the warping resistance. This effect becomes more

pronounced for specimens failing at higher stresses in the inelastic range. To take into account these enhanced corner properties, the cross-sectional properties I_x, I_y, A, J and C_ω were recalculated, where the corners were given an equivalent increased thickness t_{eq}:

$$t_{eq} = \frac{E_{tc}}{E_t} t \tag{55}$$

In the above Eq. (53), E_t is the tangent modulus of the material constituting the flat segments of the cross-section, while E_{tc} is the tangent modulus of the rounded corner material, calculated at the same strain value. The Ramberg-Osgood parameters necessary to calculate E_{tc} were obtained from Lecce (2006): $\sigma_{0.2\%}$ = 571 MPa and n = 4. Iterative calculations are necessary to ensure E_t is calculated at the buckling stress. Figure 12 displays the results of these calculations in solid line. The inelastic local buckling stress of the cross-section, which was calculated using the method set out by Becque et al. (2011), is also indicated. It is seen that good agreement is obtained between the predictions of Eq. (53), taking into account the enhanced corners, and the experimental data, up to a stress level slightly below the inelastic local buckling load. Above this level, local-overall interaction buckling becomes the governing failure mode, which cannot be accounted for using this column theory. The average ration of predicted to experimental load is 1.00 for the specimens failing in pure flexural-torsional buckling.

CONCLUSIONS

The paper presents the differential equations governing flexural, torsional and flexural-torsional buckling of inelastic columns. The theory is consistent with the principles of plastic flow theory and avoids the plastic buckling paradox by deriving an expression for the inelastic shear stiffness while considering an infinitesimal solid element transitioning to its shear-deformed state.

The theory is verified against experimental data available in literature, including examples of the pure flexural and pure torsional buckling modes of columns with a doubly symmetric cross-section, as well as examples of the flexural and flexural-torsional buckling modes of columns with a singly symmetric cross-section. Good agreement between the theory and the experiment is observed over the whole range of buckling modes.

REFERENCES

Batdorf, S.B. (1949). "Theories of Plastic Buckling." *Journal of the Aeronautical Sciences*, July, 404-408.

Bazant, Z.P., and Cedolin, L. (1991). *Stability of Structures*, Oxford University Press, Oxford, U.K.

Becque, J. (2009). "Experimental Investigation of Local-Overall Interaction Buckling of Stainless Steel Lipped Channel Columns." *Journal of Constructional Steel Research*, 65, 1677-1684.

Becque, J. (2010). "Inelastic Plate Buckling" *Journal of Engineering Mechanics*, ASCE, 136(9), 1123-1130.

Becque, J., Lathourakis, P., and Jones, R. (2011). "Experimental verification of an inelastic plate theory based on plastic flow theory." *Thin-Walled Structures*, 49(12), 1563-1572.

Bleich, H., and Bleich, F. (1936). "Biegung, Drillung und Knickung von Stäben aus Dünnen Wänden." Vorbericht zum 2. Kongress der Internazionalen Vereinigung für Brücken- und Hochbau. Verlag Ernst & Sohn, Berlin.

Considère, A. (1891). "Resistance des pièces comprimées." Congrès international des procédés de construction, Paris, Vol. 3, p. 371.

Drucker, D.C. (1950). "Some Implications of Work Hardening and Ideal Plasticity." *Quarterly of Applied Mathematics* 7, p. 411-418.

Engesser, F. (1889). *Zeitschrift fur Architektur und Ingenieurwesen,* 35, 455.

Engesser, F. (1895). *Schweizerische Bauzeitung,* 26, 24.

Gonçalves, R., and Camotim, D. (2007). "Thin-walled member plastic bifurcation analysis using generalised beam theory." *Advances in Engineering Software*, 38, pp. 637-646.

Goodier, J.N. (1942). "Flexural-Torsional Buckling of Bars of Open Section." *Cornell University Engineering Experiment Station Bulletin*, 28, 16p.

Heimerl, G.J., and Roy, J.A. (1945). "Column and Plate Compressive Strengths of Aircraft Structural Materials – Extruded 75S-T Aluminum Alloy" *NACA Wartime Report*, originally issued as Advance Restricted Report L5F08a.

Holt, M., and Leary, J.R. (1946). "The Column Strength of Aluminum Alloy 75S-T Extruded Shapes." *NACA Technical Note No. 1004*.

Hopperstad, O.S., Langseth, M., and Tryland, T. (1999). "Ultimate Strength of Aluminium Alloy Outstands in Compression: Experiments and Simplified Analysis." *Thin-Walled Structures*, 34, 279-294.

Hutchinson, J.W. (1974). "Plastic Buckling." *Advances in Applied Mechanics*, C-S. Yih, ed., Academic, New York, 67-144.

Hutchinson, J.W., and Budiansky, B. (1976). "Analytical and Numerical Study of the Effects of Initial Imperfections on the Inelastic Buckling of a Cruciform Column." *Buckling of Structures, Proceedings of the IUTAM Symposium, Cambridge, Massachussets*, B. Budiansky, editor, Springer, Berlin, 98-105.

Ilyushin, A.A. (1947). "The Elasto-Plastic Stability of Plates." *NACA Technical Note No. 1188.*

Johnson, A., and Winter, G.. (1966). "Behaviour of Stainless Steel Columns and Beams." *Journal of Structural Engineering, American Society of Civil Engineers, ASCE* 92(ST5), 97-118.

Kappus, R. (1937) "Drillknicken zentrisch gedruckter Stabe mit offenem Profil im elastischen Bereich." *Luftfahrtforschung*, 14 (9), 444-457 (translated into *NACA Technical Memorandum No. 851* (1938)).

Leary, J.R., and Holt, M. (1946). "Column Strength of Aluminum Alloy 14S-T Extruded Shapes and Rod." *NACA Technical Note No. 1027*.

Lecce, M. (2006). *Distortional Buckling of Stainless Steel Sections.* PhD Thesis, School of Civil Engineering, University of Sydney, Sydney.

Lubliner, J. (1990). *Plasticity Theory*, Macmillan, New York.

Onat, E.T., and Drucker, D.C. (1953). "Inelastic Instability and Incremental Theories of Plasticity." *Journal of the Aeronautical Sciences*, 20(3), 181-186.

Osgood, W.R., and Holt, M. (1938). "The Column Strength of Two Extruded Aluminum-Alloy H-Sections." *NACA Technical Report No. 656*.

Ramberg, W., and Osgood, W.R. (1943). *NACA Technical Note No. 902*.

Rasmussen, K.J.R., and Hancock, G.J. (1993). "Design of Cold-Formed Stainless Steel Tubular Members. I: Columns." *Journal of Structural Engineering*, 119(8), 2349-2367.

Rønning, L., Hopperstad, O.S., and Larsen, P.K. (2010). "Numerical study of the effects of constitutive models on plastic buckling of plate elements." *European Journal of Mechanics A/Solids*, 29, pp. 508-522.

Ruocco, E. (2015). "Elastoplastic buckling analysis of thin-walled structures." *Aerospace Science and Technology*, 43, pp. 176-190.

Shamass, R., Alfano, G., and Guarracino, F. (2015). "An investigation into the plastic buckling paradox for circular cylindrical shells under non-proportional loading." *Thin-Walled Structures*, 95, pp. 347-362.

Shanley, F. (1947). "Inelastic Column Theory." *Journal of the Aeronautical Sciences*, 14(5), 261-276.

Timoshenko, S.P. (1945). "Theory of Bending, Torsion and Buckling of Thin-Walled Members of Open Cross-Section." *Journal of the Franklin Institute*, 239(5), 343-361.

Timoshenko, S.P., and Gere, J.M. (1961). *Theory of Elastic Stability*, 2nd edition, McGraw-Hill, New York.

van den Berg, G.J. (1988). "The Torsional-Flexural Buckling Strength of Cold-Formed Stainless Steel Columns." *Proceedings of the Ninth International Specialty Conference on Cold-Formed Steel Structures*, Missouri-Rolla, eds. Yu, W.W., and Senne, J.H.

van den Berg, G.J. (2000). "The Effect of the Non-Linear Stress-Strain Behaviour of Stainless Steel on Member Capacity." *Journal of Constructional Steel Research*, 54(1), 135-160.

Wagner, H., and Pretschner, W. (1936). *Luftfahrtforschung*, 11, 174-180 (translated into *NACA Technical Memorandum No. 784*).

Wang, C.M., and Tun Myint Aung (2007). "Plastic buckling analysis of thick plates using p-Ritz method" *International Journal of Solids and Structures*, 44, 6239-6255.

Wang, C.M., Xiang, Y., and Chakrabarty, J. (2001). "Elastic/plastic buckling of thick plates." *International Journal of Solids and Structures*, 38, 8617-8640.

Wang, X., and Huang, J. (2009). “Elastoplastic buckling analyses of rectangular plates under biaxial loadings by the differential quadrature method.” *Thin-Walled Structures*, 47, 14-20.

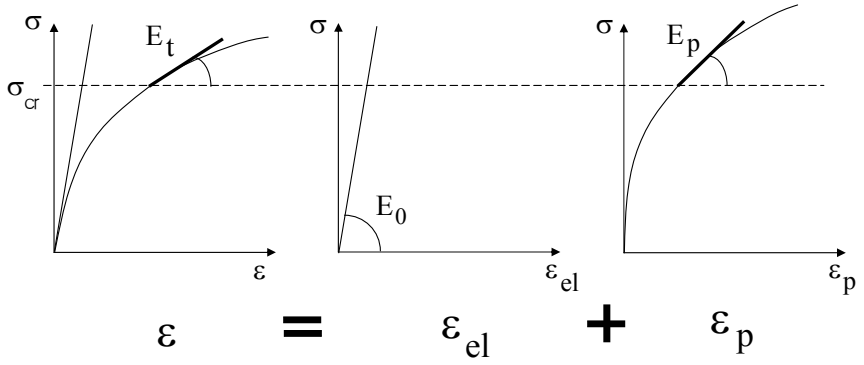

Figure 1. Material stress-strain curve

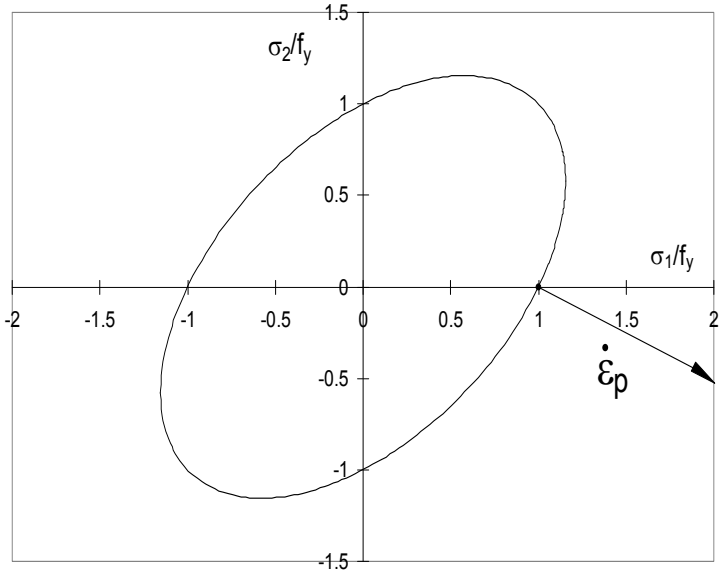

Figure 2. von Mises surface

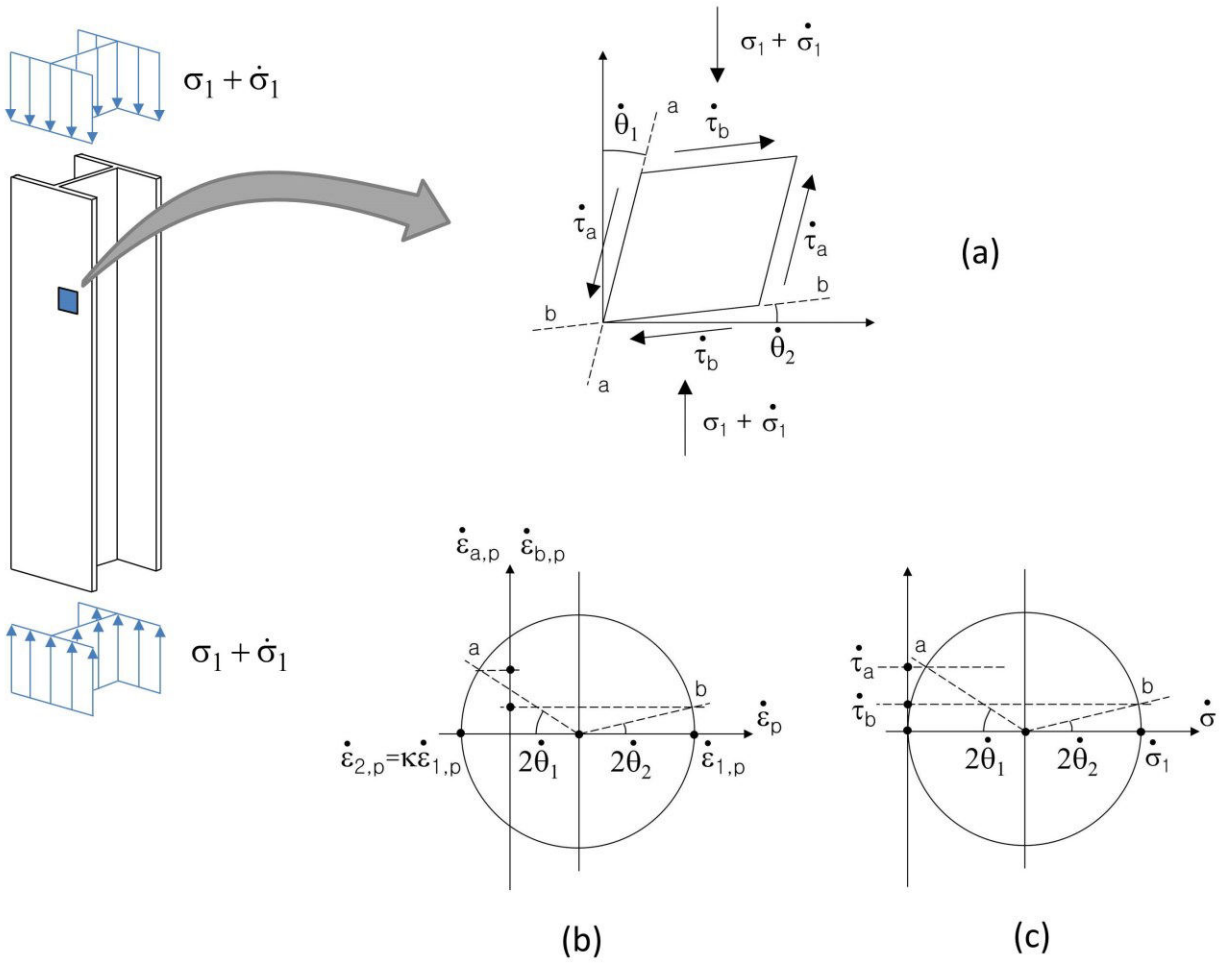

Figure 3. a. Infinitesimal element within the column, b. Mohr's circle of incremental plastic strain, c. Mohr's circle of incremental stress

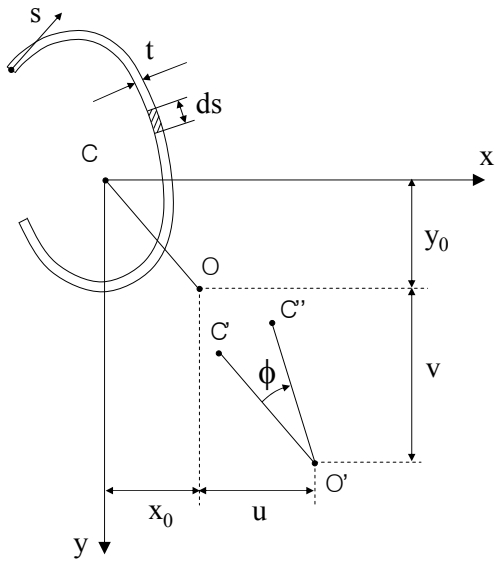

Figure 4. Column cross-section

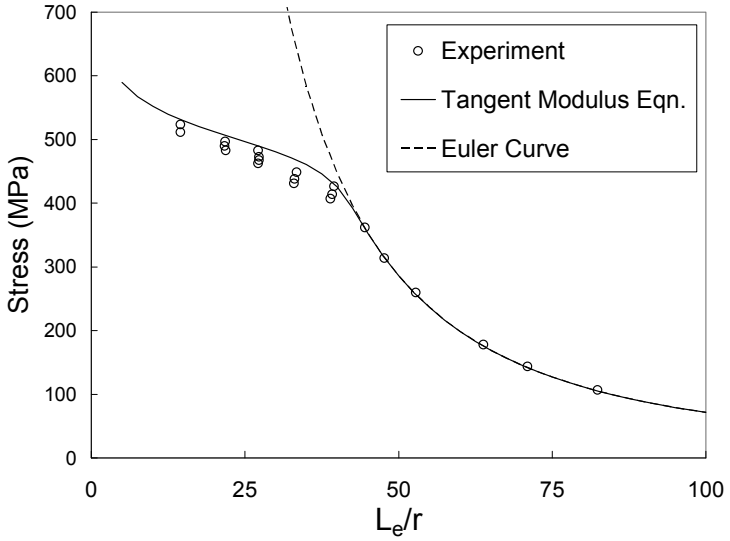

Figure 5. Tangent modulus curve vs. flexural buckling stress

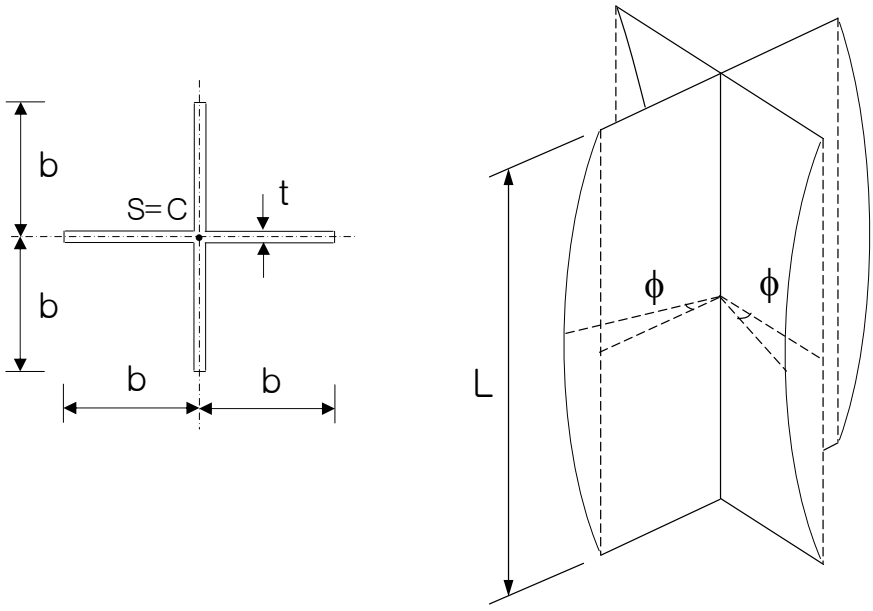

Figure 6. Torsional buckling of a cruciform column

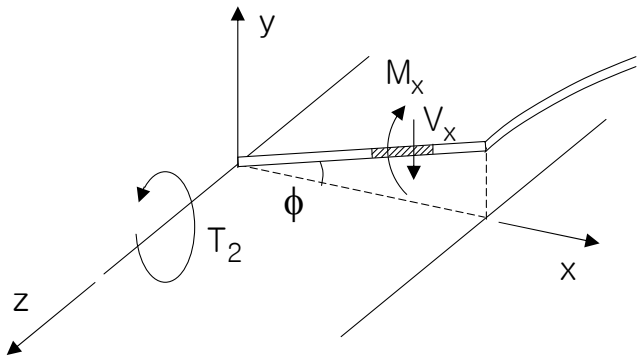

Figure 7. Flange in deformed state

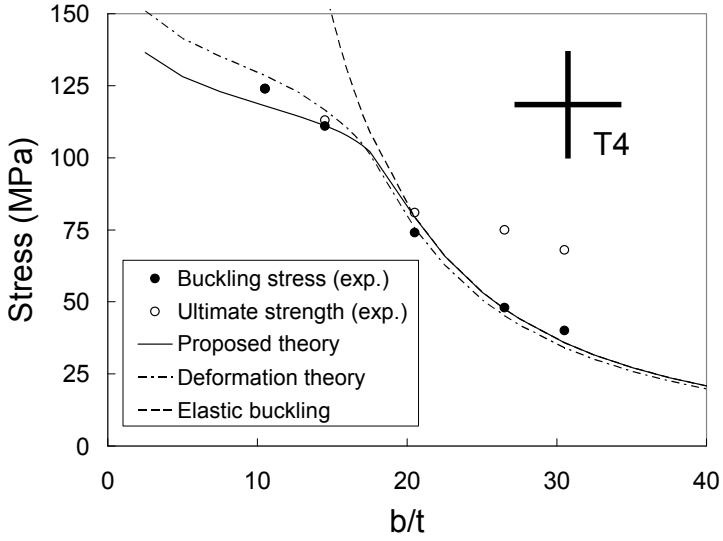

Figure 8. Torsional buckling of a cruciform section (AA6082-T4)

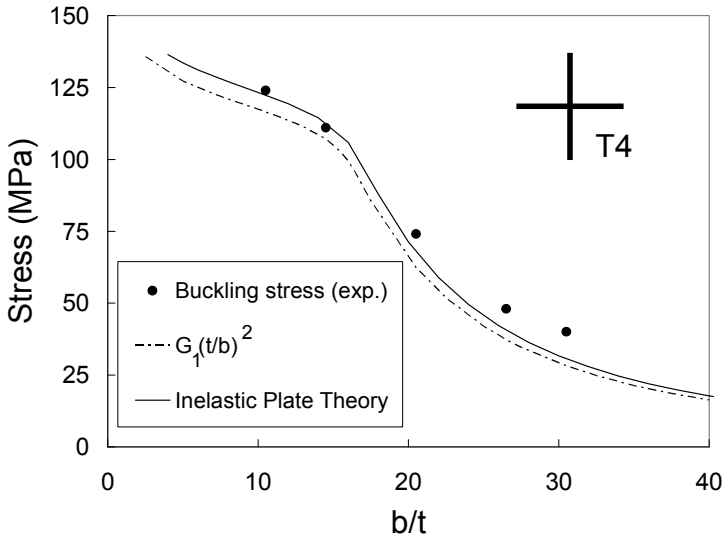

Figure 9. Approximate solutions for the cruciform column buckling problem

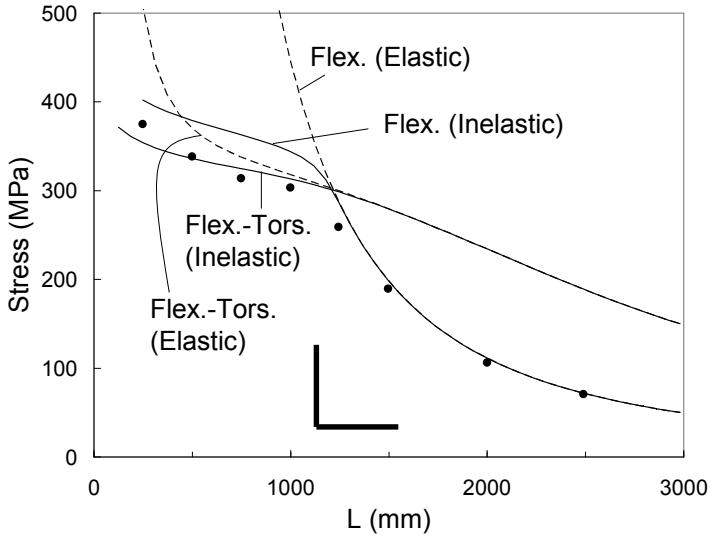

Figure 10. Flexural-torsional buckling of aluminium angles

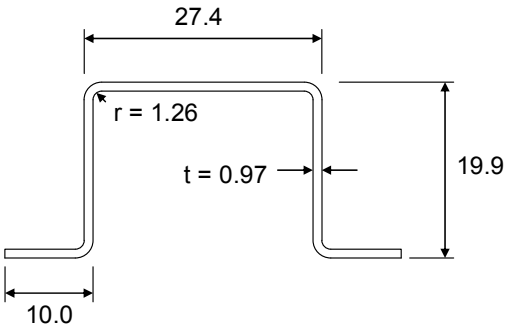

Figure 11. Hat section dimensions (in mm)

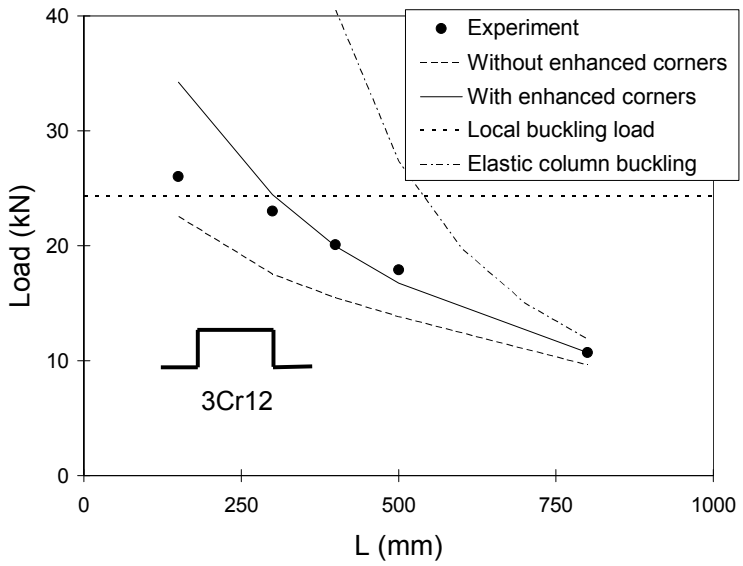

Figure 12. Flexural-torsional buckling of a hat section column